9TH INTERNATIONAL SYMPOSIUM ON PARTICLE IMAGE VELOCIMETRY – PIV'11
Kobe, Japan, July 21-23, 2011

Dynamic four-dimensional X-ray PIV of the lung

S. Dubsky[1,2], S.B. Hooper[3], K.K.W. Siu[4], A. Fouras[1]

[1]Division of Biological Engineering, Monash University, 3800, Australia
Stephen.Dubsky@monash.edu

[2]Department of Mechanical & Aerospace Engineering, Monash University, 3800, Australia

[3]Monash Institute for Medical Research, Monash University, 3800, Australia

[4]School of Physics, Monash University, 3800, Australia

ABSTRACT

During breathing, lung inflation is a dynamic process involving a balance of mechanical factors, including trans-pulmonary pressure gradients, tissue compliance and airway resistance. As breathing is a subconscious, natural act that must occur regularly to sustain life, this system must be both robust and stable. Current techniques lack the capacity for dynamic measurement of ventilation *in vivo* at sufficient spatial and temporal resolution to allow the spatio-temporal patterns of ventilation to be precisely defined. As a result, little is known of the regional lung inflation sequence. We have combined synchrotron-based imaging and dynamic computed tomography with cross-correlation velocimetry to measure 3D lung tissue motion within the mammalian lung *in vivo*. We expect that the techniques developed in this study will aid further investigation into normal and pathological lung mechanics.

1. INTRODUCTION

Studies into lung function have focused on regional differences in ventilation, but little is known about the temporal patterns of inflation. Spatial variation in mechanical properties, such as airway resistance, lung tissue compliance, and differential compliance of chest-wall components, affects both the degree of regional ventilation and the temporal filling patterns. Furthermore, these two outcomes may interact, with changes in the timing of inflation influencing *in vivo* regional ventilation.

The lack of experimental research into dynamic lung function is due to the inability of current measurement techniques to provide adequate temporal and spatial resolution to accurately characterize the precise filling patterns within the lung. Global techniques such as spirometry and gas wash-out methods offer high temporal resolution but yield little spatial information. Electrical impedance tomography [1-3] suffers from poor spatial resolution, is unable to provide morphological information, and is typically limited to measurements within a 2D plane. Magnetic resonance imaging [4, 5] and positron emission tomography [6, 7] have been used for 3D lung imaging and also motion measurement; however, both suffer from relatively poor spatial and temporal resolution, and require the introduction of contrast agents [8].

Computed tomography (CT) has long been the gold standard for high-resolution medical imaging, and is typically performed on static samples to reduce motion artefacts. Thus, application to lung function, which is inherently characterized by lung motion, has been hindered by a lack of temporal resolution. Regional expansion has been measured by registration-based techniques [9-12]. However, due to the lack of dynamic imaging capacity, these studies have resorted to inferring information from static breath-hold images, which are unlikely to contain information on the dynamics of pulmonary function. Clinical 4D-CT techniques have been recently developed to dynamically image the human lung for radiotherapy planning applications. Nevertheless, these studies have achieved a temporal resolution of 0.4s at best [13, 14], and have not investigated the temporal patterns of inflation.

Synchrotron X-ray sources, due to their brightness and coherence, are able to provide dynamic, high-resolution imaging of the lung during breathing through the use of phase contrast imaging [15, 16]. Lung tissue is an ideal sample for this technology, consisting of small air-filled sacs surrounded by soft tissue. This structure provides many air-tissue interfaces, which exhibit a sharp refractive index gradient, on which the edge enhancement of phase contrast imaging is most effective.

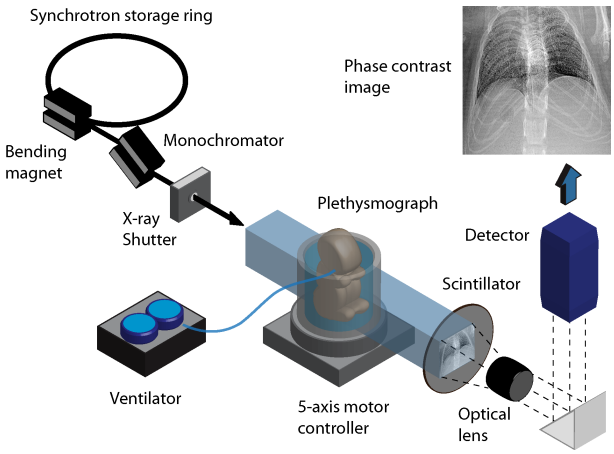

Figure 1. Schematic of the experimental setup. Monochromatic X-rays transmit through the sample and are converted into visible light by the scintillator, which imaged using conventional optics and camera.

We have developed and implemented *in vivo*, dynamic CT of the lung by utilising the advantages of synchrotron phase-contrast imaging. The high signal-to-noise ratio achieved by phase contrast, combined with the brightness of the synchrotron X-ray source, resulted in imaging of the lung at faster than video-rates. We combined this imaging with CT reconstruction to provide dynamic four-dimensional imaging

of the lung. A cross-correlation velocimetry analysis technique, based on particle image velocimetry (PIV), was used to measure lung tissue motion throughout the ventilation cycle.

The newly developed technique was applied to the measurement of lung motion in mechanically ventilated newborn rabbits using the medical imaging beamline BL20B2 at the SPring-8 Synchrotron, Japan. Using this data, we have identified spatial and temporal patterns of motion.

2. METHODS

2.1 Four-dimensional computed tomography

The dynamic CT was conducted at the BL20B2 beamline at the SPring-8 Synchrotron, Japan. All procedures were approved by the SPring-8 Synchrotron Facility and Monash University's School of Biomedical Science's Animal Ethics Committees. The imaging setup is presented in Figure 1. A custom designed ventilator [17] capable of stable, repeatable ventilation was used to ventilate the animal. Conventional positive pressure ventilation was used, with inspiration and expiration times of 1s and 1.5s respectively. Inspiratory and expiratory pressures were 27mmH_2O and 5mmH_2O respectively. Images were acquired at 20 time points within the breathing cycle: 10 during inspiration, and 10 during expiration, triggered at the start of inspiration and expiration respectively and at a rate of 34.5 fps. Images were acquired using a Hamamatsu X-ray converter equipped with an EMCCD detector (C9100-02). Details of the imaging setup and animal handling procedure have been reported elsewhere [16, 18]. The animal was rotated through 180 degrees, and phase contrast images acquired over 406 breaths, allowing reconstruction of the three-dimensional morphology (Figure 2) of the lung at 20 time points within the breathing cycle. The reconstructions were performed using an algebraic reconstruction technique.

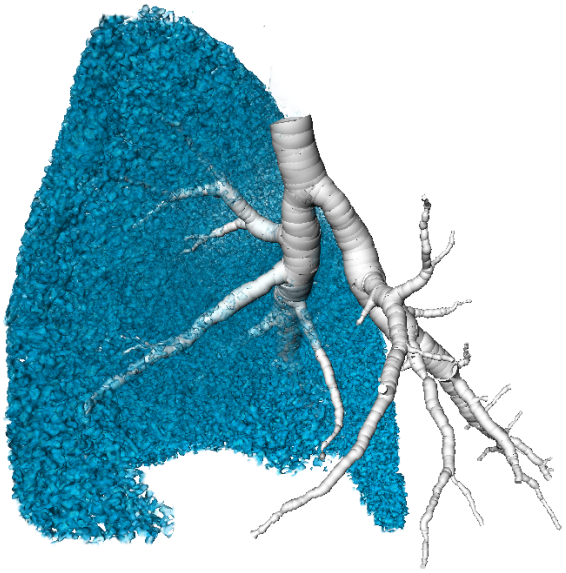

Figure 2. Computed tomographic reconstruction of the lung. Only the right lung is shown (blue) to allow visualisation of the segmented airway tree (rendered in white).

2.2 Lung tissue motion measurement

The motion of the lung tissue during the ventilation cycle was calculated using a technique based on particle image velocimetry (PIV). PIV is routinely used in fluid mechanics studies to accurately measure the velocity of tracer particles within a fluid flow, traditionally in two dimensions [19], but recently has been expanded to 3D [20]. Lung tissue is well suited to this form of analysis as it consists of many small airsacs, providing a high density of information with which to track the motion.

The cross-correlation analysis was performed in three-dimensions. The images were discretised into cubes of 64×64×64 voxels, with a spacing of 8 voxels on a regular grid, and cross-correlation performed on these regions between consecutive images. An iterative approach was used, whereby the first iteration provides an estimate of the displacement, and subsequent iterations are performed with the second image region being offset by this estimate, reducing the errors associated with parts of tissue leaving the interrogation region. The universal outlier detection method [21] was employed to eliminate errors due to spurious measurements.

3. RESULTS

Dynamic computed tomography yielded morphological and tissue motion data at 20 phases within the ventilation cycle. Figure 3 shows maps of lung tissue velocity at 4 time points (out of 20) during inflation; measured by the cross-correlation analysis. Initially, the lungs expand outwards from the centre of the chest (Figure 3A and 3B). Once the upper regions of the lung become fully inflated, the lower lung tissue continues to displace down into the base of the chest cavity (Figure 3C and 3D). The sequence is repeated during expiration, with the base of the lung continuing to displace upwards after the apex has become stationary.

4. DISCUSSION AND CONCLUSIONS

Temporal patterns of inflation play an important role in lung mechanics. The time scale of inflation variations within the lungs is small (on the order of ms), and the results found in this study would be unobtainable using the previously available techniques. We have developed the capacity not only to measure dynamic regional motion of lung tissue, but also to measure the airway tree geometry. The quantitative motion measurements available using the newly developed technique offer the potential for further analysis to calculate regional expansion and ventilation. This capacity, combined with airway geometry measurement could provide experimental data on the effects of airway geometry on regional airflow distributions *in vivo*, where studies were previously limited to numerical simulation [12, 22]. Furthermore, this information can be used for validation of numerical studies, and to provide data for the determination of boundary conditions.

The dynamic measurement methods developed in this study are applicable to a wide range of lung mechanics problems, particularly those where temporal patterns are important, such as in high-frequency oscillatory ventilation studies [23]. Another enticing application for these techniques lies in the diagnosis and study of lung pathology. For example, lung diseases that alter the lung tissue structure or airway calibre, such as cancer [24, 25] and asthma [7, 8, 26] may dramatically affect the temporal inflation patterns, and so motion measurement could provide a more sensitive indicator than regional ventilation measures.

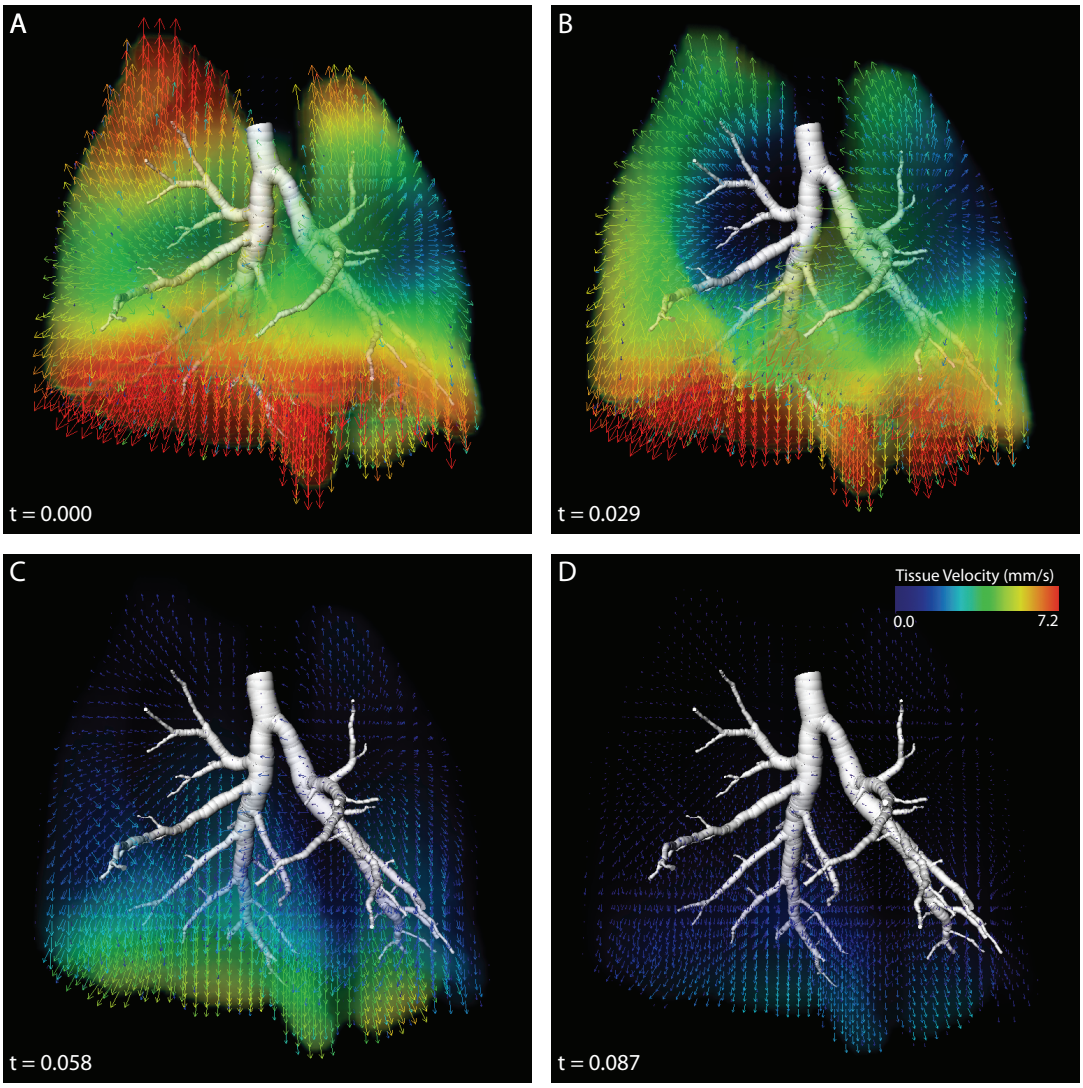

Figure 3. Three-dimensional maps of lung tissue velocity for 4 time points during inspiration, as measured using PIV. Vectors represent tissue velocity. Colours represent velocity magnitude, and segmented airway tree is rendered uncoloured.

ACKNOWLEDGMENTS

We acknowledge the support of the Australian Research Council; the National Health and Medical Research Council; Japan Synchrotron Radiation Research Institute (JASRI); and the American Asthma Foundation. We thank K. Uesugi, N. Yagi, M.J. Wallace, B.J.Allison and K.Wheeler for assistance with experiments and D. Lo Jacono for discussions.

REFERENCES

[1] Frerichs, I., *Electrical impedance tomography (EIT) in applications related to lung and ventilation: a review of experimental and clinical activities.* Physiological Measurement, 2000. **21**(2): p. R1-R21.

[2] Metherall, P., D.C. Barber, R.H. Smallwood, and B.H. Brown, *Three-dimensional electrical impedance tomography.* Nature, 1996. **380**(6574): p. 509-512.

[3] Victorino, J.A., J.B. Borges, V.N. Okamoto, G.F.J. Matos, M.R. Tucci, M.P.R. Caramez, H. Tanaka, F.S. Sipmann, D.C.B. Santos, C.S.V. Barbas, C.R.R. Carvalho, and M.B.P. Amato, *Imbalances in regional lung ventilation - A validation study on electrical impedance tomography.* American Journal of Respiratory and Critical Care Medicine, 2004. **169**(7): p. 791-800.

[4] Albert, M.S., G.D. Cates, B. Driehuys, W. Happer, B. Saam, C.S. Springer, and A. Wishnia, *Biological Magnetic-Resonance-Imaging Using Laser Polarized Xe-129.* Nature, 1994. **370**(6486): p. 199-201.

[5] Ebert, M., T. Grossmann, W. Heil, W.E. Otten, R. Surkau, M. Leduc, P. Bachert, M.V. Knopp, L.R. Schad, and M. Thelen, *Nuclear magnetic resonance imaging with hyperpolarised helium-3.* Lancet, 1996. **347**(9011): p. 1297-1299.

[6] Musch, G., J.D.H. Layfield, R.S. Harris, M.F.V. Melo, T. Winkler, R.J. Callahan, A.J. Fischman, and J.G. Venegas, *Topographical distribution of pulmonary perfusion and ventilation, assessed by PET in supine and prone humans.* Journal of Applied Physiology, 2002. **93**(5): p. 1841-1851.

[7] Venegas, J.G., T. Winkler, G. Musch, M.F.V. Melo, D. Layfield, N. Tgavalekos, A.J. Fischman, R.J. Callahan, G. Bellani, and R.S. Harris, *Self-organized patchiness in asthma as a prelude to catastrophic shifts.* Nature, 2005. **434**(7034): p. 777-782.

[8] Jannasch, K., J. Missbach-Guentner, and F. Alves, *Using in vivo imaging for asthma.* Drug Discovery Today: Disease Models, 2009. **6**(4): p. 129-135.

[9] Christensen, G.E., J.H. Song, W. Lu, I. El Naqa, and D.A. Low, *Tracking lung tissue motion and expansion/compression with inverse consistent image registration and spirometry.* Medical Physics, 2007. **34**(6): p. 2155-2163.

[10] Ding, K., J.E. Bayouth, J.M. Buatti, G.E. Christensen, and J.M. Reinhardt, *4DCT-based measurement of changes in pulmonary function following a course of radiation therapy.* Medical Physics, 2010. **37**(3): p. 1261-1272.

[11] Reinhardt, J.M., K. Ding, K. Cao, G.E. Christensen, E.A. Hoffman, and S.V. Bodas, *Registration-based estimates of local lung tissue expansion compared to xenon CT measures of specific ventilation.* Medical Image Analysis, 2008. **12**(6): p. 752-763.

[12] Yin, Y.B., J.W. Choi, E.A. Hoffman, M.H. Tawhai, and C.L. Lin, *Simulation of pulmonary air flow with a subject-specific boundary condition.* Journal of Biomechanics, 2010. **43**(11): p. 2159-2163.

[13] Guerrero, T., K. Sanders, E. Castillo, Y. Zhang, L. Bidaut, T.S. Pan, and R. Komaki, *Dynamic ventilation imaging from four-dimensional computed tomography.* Physics in Medicine and Biology, 2006. **51**(4): p. 777-791.

[14] Zhao, T.Y., W. Lu, D.S. Yang, S. Mutic, C.E. Noel, P.J. Parikh, J.D. Bradley, and D.A. Low, *Characterization of free breathing patterns with 5D lung motion model.* Medical Physics, 2009. **36**(11): p. 5183-5189.

[15] Fouras, A., M.J. Kitchen, S. Dubsky, R.A. Lewis, S.B. Hooper, and K. Hourigan, *The past, present, and future of x-ray technology for in vivo imaging of function and form.* Journal of Applied Physics, 2009. **105**(10): p. 102009.

[16] Lewis, R.A., N. Yagi, M.J. Kitchen, M.J. Morgan, D. Paganin, K.K.W. Siu, K. Pavlov, I. Williams, K. Uesugi, M.J. Wallace, C.J. Hall, J. Whitley, and S.B. Hooper, *Dynamic imaging of the lungs using x-ray phase contrast.* Physics in Medicine and Biology, 2005. **50**(21): p. 5031-5040.

[17] Kitchen, M.J., A. Habib, A. Fouras, S. Dubsky, R.A. Lewis, M.J. Wallace, and S.B. Hooper, *A new design for high stability pressure-controlled ventilation for small animal lung imaging.* Journal of Instrumentation, 2010. **5**: p. T02002.

[18] Kitchen, M.J., R.A. Lewis, M.J. Morgan, M.J. Wallace, M.L. Siew, K.K.W. Siu, A. Habib, A. Fouras, N. Yagi, K. Uesugi, and S.B. Hooper, *Dynamic measures of regional lung air volume using phase contrast x-ray imaging.* Physics in Medicine and Biology, 2008. **53**(21): p. 6065-6077.

[19] Adrian, R.J., *Particle-Imaging Techniques for Experimental Fluid-Mechanics.* Annual Review of Fluid Mechanics, 1991. **23**: p. 261-304.

[20] Elsinga, G.E., F. Scarano, B. Wieneke, and B.W. van Oudheusden, *Tomographic particle image velocimetry.* Experiments in Fluids, 2006. **41**(6): p. 933-947.

[21] Westerweel, J. and F. Scarano, *Universal outlier detection for PIV data.* Experiments in Fluids, 2005. **39**(6): p. 1096-1100.

[22] Mauroy, B., M. Filoche, E.R. Weibel, and B. Sapoval, *An optimal bronchial tree may be dangerous.* Nature, 2004. **427**(6975): p. 633-636.

[23] Habib, R.H. and R.A. Assaly, *Dynamic respiratory mechanics measurements for optimization of ventilator settings in acute lung injury.* Critical Care Medicine, 2007. **35**(7): p. 1806-1807.

[24] Kerr, K.M., *Pulmonary adenocarcinomas: classification and reporting.* Histopathology, 2009. **54**(1): p. 12-27.

[25] Noguchi, M., A. Morikawa, M. Kawasaki, Y. Matsuno, T. Yamada, S. Hirohashi, H. Kondo, and Y. Shimosato, *Small Adenocarcinoma of the Lung - Histologic Characteristics and Prognosis.* Cancer, 1995. **75**(12): p. 2844-2852.

[26] Faffe, D.S. and W.A. Zin, *Lung Parenchymal Mechanics in Health and Disease.* Physiological Reviews, 2009. **89**(3): p. 759-775.